Pluripotent stem cell derived dopaminergic subpopulations model the selective neuron degeneration in Parkinson's disease

Tony Oosterveen,[1,6] Pedro Garção,[1,6] Emma Moles-Garcia,[1,6] Clement Soleilhavoup,[1] Marco Travaglio,[1] Shahida Sheraz,[3] Rosa Peltrini,[1] Kieran Patrick,[1] Valerie Labas,[2] Lucie Combes-Soia,[2] Ulrika Marklund,[4] Peter Hohenstein,[3,5] and Lia Panman[1,*]

[1]MRC Toxicology Unit, University of Cambridge, Tennis Court Road, Cambridge CB2 1QR, UK
[2]PRC, INRA, CNRS, University of Tours, IFCE, Nouzilly, France
[3]Roslin Institute, University of Edinburgh, Edinburgh, UK
[4]Department of Medical Biochemistry and Biophysics, Karolinska Institute, Stockholm, Sweden
[5]Present address: Leiden University Medical Center, Leiden, the Netherlands
[6]These authors contributed equally
*Correspondence: liapanman1@gmail.com
https://doi.org/10.1016/j.stemcr.2021.09.014

SUMMARY

In Parkinson's disease (PD), substantia nigra (SN) dopaminergic (DA) neurons degenerate, while related ventral tegmental area (VTA) DA neurons remain relatively unaffected. Here, we present a methodology that directs the differentiation of mouse and human pluripotent stem cells toward either SN- or VTA-like DA lineage and models their distinct vulnerabilities. We show that the level of WNT activity is critical for the induction of the SN- and VTA-lineage transcription factors *Sox6* and *Otx2*, respectively. Both WNT signaling modulation and forced expression of these transcription factors can drive DA neurons toward the SN- or VTA-like fate. Importantly, the SN-like lineage enriched DA cultures recapitulate the selective sensitivity to mitochondrial toxins as observed in PD, while VTA-like neuron-enriched cultures are more resistant. Furthermore, a proteomics approach led to the identification of compounds that alter SN neuronal survival, demonstrating the utility of our strategy for disease modeling and drug discovery.

INTRODUCTION

Pluripotent stem cells (PSCs) are an important tool for disease modeling and drug-screening approaches. Several methodologies have been developed to generate neurons implicated in neurodegenerative disease such as dopaminergic, motor, and striatal projection neurons (Tao and Zhang, 2016). Substantia nigra (SN) dopaminergic neurons (DA) are highly susceptible to genetic and environmental toxicity, leading to their selective degeneration in Parkinson's disease (PD). In contrast, the related ventral tegmental area (VTA) DA neurons are more resistant to these insults (Surmeier et al., 2017). Access to PSC-derived cultures enriched for distinct DA subpopulations is an attractive approach to model the selective cell death of SN neurons in PD.

Midbrain DA (mDA) neurons are derived from midbrain floor-plate (FP) cells that are specified by Sonic Hedgehog (SHH), fibroblast growth factor 8 (FGF8), and WNT signaling during embryonic development (Smidt and Burbach, 2007). In several studies the timely addition of developmental relevant signaling molecules resulted in the efficient generation of functional mDA neurons from mouse and human PSCs (Kirkeby et al., 2012; Kriks et al., 2011; Lee et al., 2000; Nolbrant et al., 2017; Ying et al., 2003). These PSC-derived DA cultures are a mixture of neurons with both SN and VTA-like identities, but their relative contribution has not been analyzed in detail. Furthermore,

subpopulation identity in these cultures was mainly based on late-onset markers that are not fully restricted to either the SN or VTA neuronal lineage (Fu et al., 2012; Reyes et al., 2012). In addition, the presence of other molecularly defined subpopulations of DA neurons (Poulin et al., 2020) has not been addressed in these cultures.

It is currently unclear how to generate DA cultures enriched for either SN or VTA neurons. The recent identification of SOX6 and OTX2 as early and selective markers of the SN and VTA neuronal lineages, respectively, demonstrated that DA subpopulation diversity is already established at neural progenitor stage, with SN neurons arising from medially located progenitors (Blaess et al., 2011; Panman et al., 2014; Poulin et al., 2014; Tiklova et al., 2019). WNT signaling plays an important role in the regulation of *Otx2* expression, which confers resistance to dopaminergic neurons and promotes VTA neuron differentiation (Di Salvio et al., 2010; Grealish et al., 2014; Prakash et al., 2006). Therefore, the early restricted expression of DA sublineage specific markers SOX6 and OTX2 suggests the requirement for optimized culture conditions that promotes the acquisition of either the SN- or VTA-specific neuronal lineage in PSC-derived progenitors.

Here we used insight from developmental studies to establish PSC differentiation conditions that promote the acquisition of SN-specific neuronal identities in mDA cultures. We show that temporal WNT signaling inhibition is required to induce medial FP precursors that are
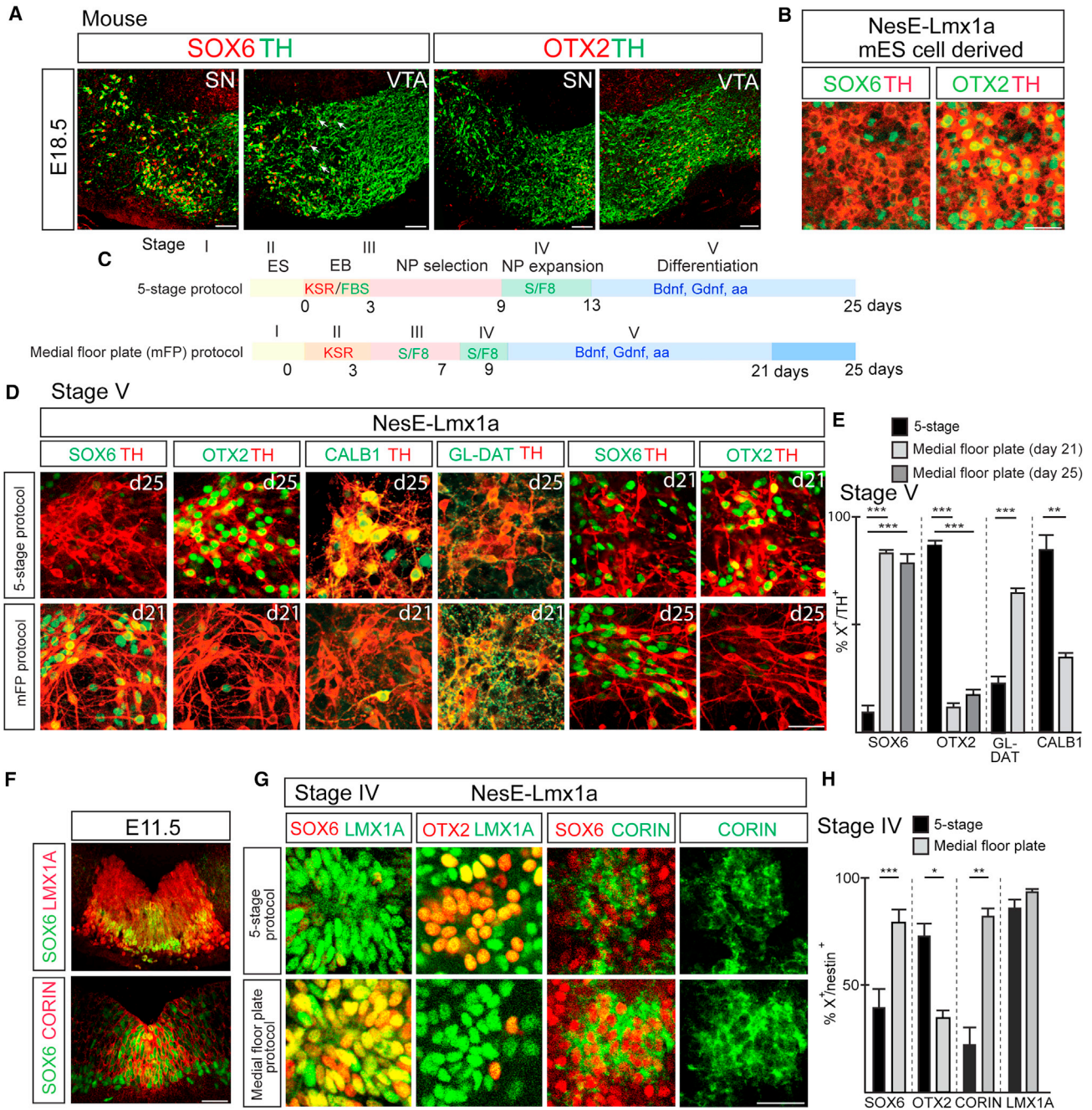
Figure 1. Directed differentiation of mESCs toward SN-like neuronal lineage

(A) Immunohistochemical (IHC) analysis of SOX6 and OTX2 in SN and VTA neurons of E18.5 mouse embryo. Arrows point to Sox6-expressing cells within VTA.

(B) IHC analysis of Nes-Lmx1a mESC-derived DA neurons.

(C) Schematic overview of the 5-stage and medial FP protocols.

(D) IHC analysis of NesE-Lmx1a ESC-derived neurons (stage V).

(E) Percentages of TH$^+$ neurons expressing the indicated neuronal markers in Nes-Lmx1a mESC-derived DA neurons (stage V). Mean values ± SD; one-way ANOVA with Bonferroni correction (SOX6 and OTX2) or unpaired t test (GlycoDAT and CALB1); n = 3 independent experiments.

(F) IHC analysis of midbrain FP of E11.5 mouse embryo.

(legend continued on next page)

efficiently directed toward the SN-like neuronal lineage. Furthermore, we demonstrate that our strategy enables the derivation of distinct DA subpopulations that are distinguishable by their selective sensitivity to mitochondrial toxicity, providing a tool to model PD *in vitro*.

RESULTS

Directing differentiation of mESC-derived medial FP precursors toward SN-like neuronal lineage

SOX6 and OTX2 are early and selective DA sublineage determinants during mouse embryonic development (Panman et al., 2014) (Figures 1A and 1F). While OTX2 is solely confined to VTA neurons, SOX6 is expressed in SN neurons, the parabrachial pigmented (PBP) part of the VTA, and the retrorubral field (RRF) (Figure 1A; Poulin et al., 2020). To investigate the early aspects of SN and VTA neuronal lineage specification during PSC differentiation, we assessed the percentage of SOX6- and OTX2-labeled DA neurons derived from wild-type and NesE-Lmx1a mouse embryonic stem cells (mESCs) (Friling et al., 2009; Panman et al., 2011) differentiated according to the 5-stage protocol as previously described (Lee et al., 2000) (Figure 1C and Table S1, protocol 3). Remarkably, only a small proportion (less than 10%) of DA neurons derived from wild-type or NesE-Lmx1a (Figures 1B, S1A, S1B, and S1F) ESC lines expressed SOX6, while the majority of the neurons (more than 80%) were OTX2 positive (Figures 1B, S1A, S1B, and S1F). Consistently, a large fraction of the neurons was positively labeled for CALBINDIN1 (CALB1) and negatively for GlycoDAT (Figure S1F), indicating that most neurons have VTA-like identities. The distinct spatial-temporal origin of DA subpopulations (Blaess et al., 2011; Panman et al., 2014) suggests that different culture conditions may be needed for inducing the SN neuronal lineage. Therefore, we decided to systematically alter several steps of the 5-stage protocol to define SN neuronal lineage-promoting conditions (see Table S1 for a summary). We replaced fetal bovine serum with knockout serum replacement (KSR) during the embryonic body (EB) formation (stage II; Figure 1C and Table S1, protocol 1), which did not alter the differentiation outcome of the 5-stage protocol, with the majority of neurons expressing VTA-specific markers (Figures 1D and 1E). However, when using KSR in combination with earlier and shorter exposure of progenitors at the neural progenitor (NP) selection stage (stage III) and NP expansion stage (stage IV) to SHH and FGF8 (S/F8), nearly all NesE-

Lmx1a mESC-derived DA neurons became SOX6 positive (83%) and there was a striking reduction in the number of OTX2-labeled DA neurons (12%) (Figures 1C–1E and Table S1, protocol 2). We termed this modified version the "medial FP (mFP) protocol," referring to the developmental origin of SN neurons. Similar results were obtained when using wild-type ESCs or a second independently generated NesE-Lmx1a ESC line (Figures S1A and S1B). Extending the mFP protocol to 25 days did not result in an increase of OTX2-expressing neurons (Figures 1D and 1E). The specification of SN-like specific neuronal identities under the mFP protocol was further supported by the increase in GLYCO-DAT-labeled (from 23% to 65%) and decrease in CALB1-labeled (from 85% to 34%) DA neurons (Figures 1D and 1E). In addition, Sox6-expressing neurons were positive for ALDH1A1 (Figure S1D), further supporting the SN-like neuronal identity. The altered culture conditions did not compromise DA cell numbers (35% TH/4′,6-diamidino-2-phenylindole [DAPI] in both 5-stage and mFP protocol) and midbrain identity as revealed by the maintenance of FOXA2, LMX1A, NR4A2, and EN1 expression (Figures S1A and S1C). Remarkably, the use of KSR during EB formation in combination with the addition of the growth factors S/F8 during the NP selection stage for 4 days (stage III) and NP expansion stage for 2 days (stage IV) are essential protocol steps for promoting SN-like subpopulation identity (Figure 1C and Table S1, protocol 2), and any variation on this protocol abolished the production of healthy-looking Sox6-expressing DA neurons (Figures S1E–S1G and Table S1).

In the medial part of the FP, SOX6-labeled cells coexpress CORIN (Figure 1F). Next, we investigated whether mFP cells are initially specified when using SN neuron-promoting culture conditions. Indeed, we observed a robust increase in SOX6-labeled (90%) and CORIN-labeled (82%) DA progenitor cells at stage IV of the mFP protocol, while the 5-stage-protocol mainly yielded the lateral OTX2-expressing DA progenitors (Figures 1G and 1H). The unaltered expression of LMX1A shows that DA progenitors are generated with similar efficiency in both protocols (Figure 1H).

Canonical WNT signaling mediates dopaminergic subpopulation diversification

By altering the timing of growth factor exposure during mESC differentiation, we were able to switch dopaminergic subpopulation identity of the obtained cultures from VTA- to SN-like. A possible explanation for this lineage switch is

---

(G) IHC analysis of DA progenitor markers in Nes-Lmx1a mESC-derived progenitors (stage IV).

(H) Percentage of NESTIN^{+} cells expressing indicated markers in Nes-Lmx1a mESC-derived neural progenitors (stage IV). n = 3 independent experiments; mean values ± SD; unpaired t test.

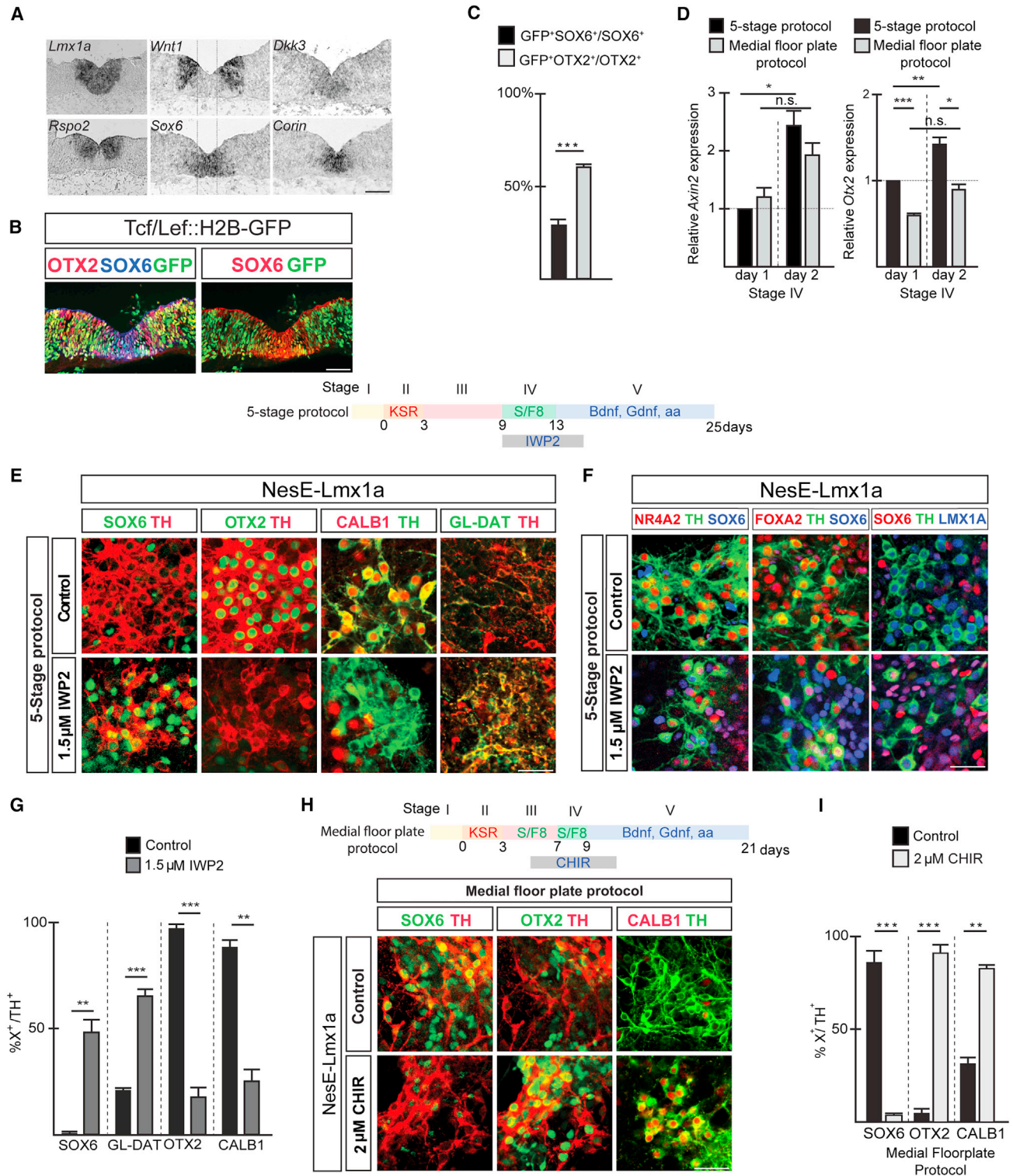*p < 0.05, **p < 0.01, ***p < 0.001. Scale bars, 100 μm (A and F) and 50 μm (B, D, and G).

Figure 2. Differential WNT signaling levels regulate DA neuronal subpopulation specification during mESC differentiation

(A) Gene expression patterns of WNT signaling components in relation to *Sox6* and *Lmx1a* in the FP of E11.5 mouse embryo.

(B) IHC analysis of the midbrain FP of Tcf/Lef::H2B-GFP reporter mouse line at E11.5. Reporter activation is visualized by GFP expression.

(legend continued on next page)

the protocol-dependent differential production of endogenous canonical WNT signaling. Expression analysis demonstrates that the WNT/β-CATENIN signaling pathway is selectively activated in OTX2^{+} lateral dopaminergic progenitors as shown by the lateral localization of *Wnt1* and *Rspo2* transcripts, the medial expression of repressors *Dkk1* (Ribeiro et al., 2011) and *Dkk3* (Nakamura and Hackam, 2010) (Figure 2A), and overlap between GFP-labeled WNT responding progenitor cells with OTX2 in the Tcf/Lef::H2B-GFP reporter mouse line. Furthermore, canonical WNT target genes *Axin2* (Jho et al., 2002) and *Otx2* (Chung et al., 2009) are higher expressed in 5-stage than in mFP-protocol-derived progenitors at days 1 and 2 of stage IV of the respective protocols (Figure 2D), indicating that production of WNT signaling could indeed be culture condition dependent. Next, we tested whether addition of canonical WNT inhibitors or activators to differentiating progenitors promotes the acquisition of SN- or VTA-like identities in dopaminergic cultures, respectively. Neural progenitors displayed expected responsiveness to WNT activator CHIR (Ying et al., 2008) and inhibitors IWP2 and IWR1 (Chen et al., 2009) as observed by up- or down-regulation of *Axin2*, respectively (Figures S1H–S1J). Five-stage protocol-derived progenitors (Figure 2E) treated for 6 days with WNT inhibitor IWP2 showed an increased percentage of SOX6- and GLYCO-DAT-labeled dopaminergic neurons and reciprocally a drastic downregulation of VTA restricted markers OTX2 and CALB1 (Figures 2E and 2G). While the selected timing and duration of IWP2 treatment had only a minor effect on dopaminergic cell numbers (32% TH/DAPI), mDA identity was preserved as shown by overlap of SOX6 with NR4A2, FOXA2, and LMX1A expression (Figure 2F). To assess whether Wnt signaling activation is sufficient to control SN- to VTA-like neuronal lineage conversion, we treated mFP-derived progenitors for 6 days with CHIR during stage III and IV (Figure 2H). This resulted in a robust decrease of SOX6- and an increase of OTX2- and CALB1-labeled dopaminergic neurons (Figures 2H and 2I), indicating that WNT activation promotes VTA neuronal lineage specification. The WNT-mediated

dopaminergic lineage switch already takes place at progenitor stage, as WNT activation and inhibition resulted in down- and upregulation, respectively of medial progenitor markers *Corin* and *Sox6* (Figure S1K).

Mitochondrial toxin exposure results in the selective degeneration of SN neurons (Bove et al., 2005). To test whether we can recapitulate the selective vulnerability of DA neurons *in vitro*, we compared the effects of mitochondrial toxins on neuronal survival between 5-stage and mFP-derived cultures (Figure 3A). The mFP protocol-derived DA cultures displayed increased sensitivity to mitochondrial toxins with a strong increase in the number of apoptotic neurons as visualized by cCASP3 labeling (Figures 3F and 3I) and a decrease in number of TH-expressing cells (Figures 3C and 3D) after treatment with MPP[+] and rotenone for 48 h. In contrast, 5-stage protocol-derived DA neurons were significantly less affected by these mitochondrial toxins (Figures 3B, 3D, 3E, and 3I). To address whether there is a direct correlation between the presence of SOX6-labeled DA neurons in cultures and increased vulnerability, we analyzed the effects of mitochondrial toxins on cell survival after manipulating SOX6 levels by Wnt signaling modulators. No effects on cell death and TH[+] cell numbers were observed after addition of Wnt signaling inhibitors and activators to differentiating cultures without toxin exposure (Figures 3A–3I). However, the IWP2-mediated induction of SOX6 in 5-stage protocol-derived cultures rendered these neurons far more sensitive to MPP[+] and rotenone, resulting in reduction of TH-labeled cells (Figures 3B and 3D) and an increase in cCASP3 expression (Figures 3E and 3I). Interestingly, reducing SOX6 expression in mFP-derived cultures by CHIR exposure (Figure 2G) reversed the effects of mitochondrial toxins on cell survival (Figures 3C, 3D, 3F, and 3I). Consistent with the increased sensitivity of SOX6-enriched DA cultures, cCASP3 expression was mainly induced in SOX6-labeled DA neurons while OTX2 DA neurons were largely unaffected (Figures 3G, 3H, 3J, and 3K). Altogether, differential levels of Wnt signaling directs DA sublineage selection and consequently determines the vulnerability of obtained cultures.

(C) Percentage GFP[+] DA neuronal progenitors expressing either SOX6 or OTX2 in the Tcf/Lef::H2B-GFP reporter mouse line. Mean values ± SD; unpaired t test; n = 3 independent experiments.
(D) qPCR analysis of *Axin2* and *Otx2* expression levels in NesE-Lmx1a ESC-derived neural progenitors at day 1 and day 2 of stage IV. n = 5 independent experiments; mean values ± SEM; two-way ANOVA with Bonferroni correction; n.s., not significant.
(E) Experimental design differentiation protocol. IHC analysis of NesE-Lmx1a ESC DA cultures (stage V).
(F) DA marker analysis of NesE-Lmx1a mESC-derived cultures differentiated according the 5-stage protocol (stage V) and treated with 1.5 μM IWP2.
(G) Percentages of TH^{+} neurons expressing the indicated markers in NesE-Lmx1a ESC-derived cultures (stage V) differentiated as described in (E). Mean values ± SD; unpaired t test; n = 3 independent experiments.
(H) Scheme of differentiation protocol. Immunohistochemical analysis of control and CHIR-treated cultures (stage V).
(I) Percentages of TH^{+} neurons expressing indicated markers differentiated as described in (H). Mean values ± SD; unpaired t test; n = 3 independent experiments.
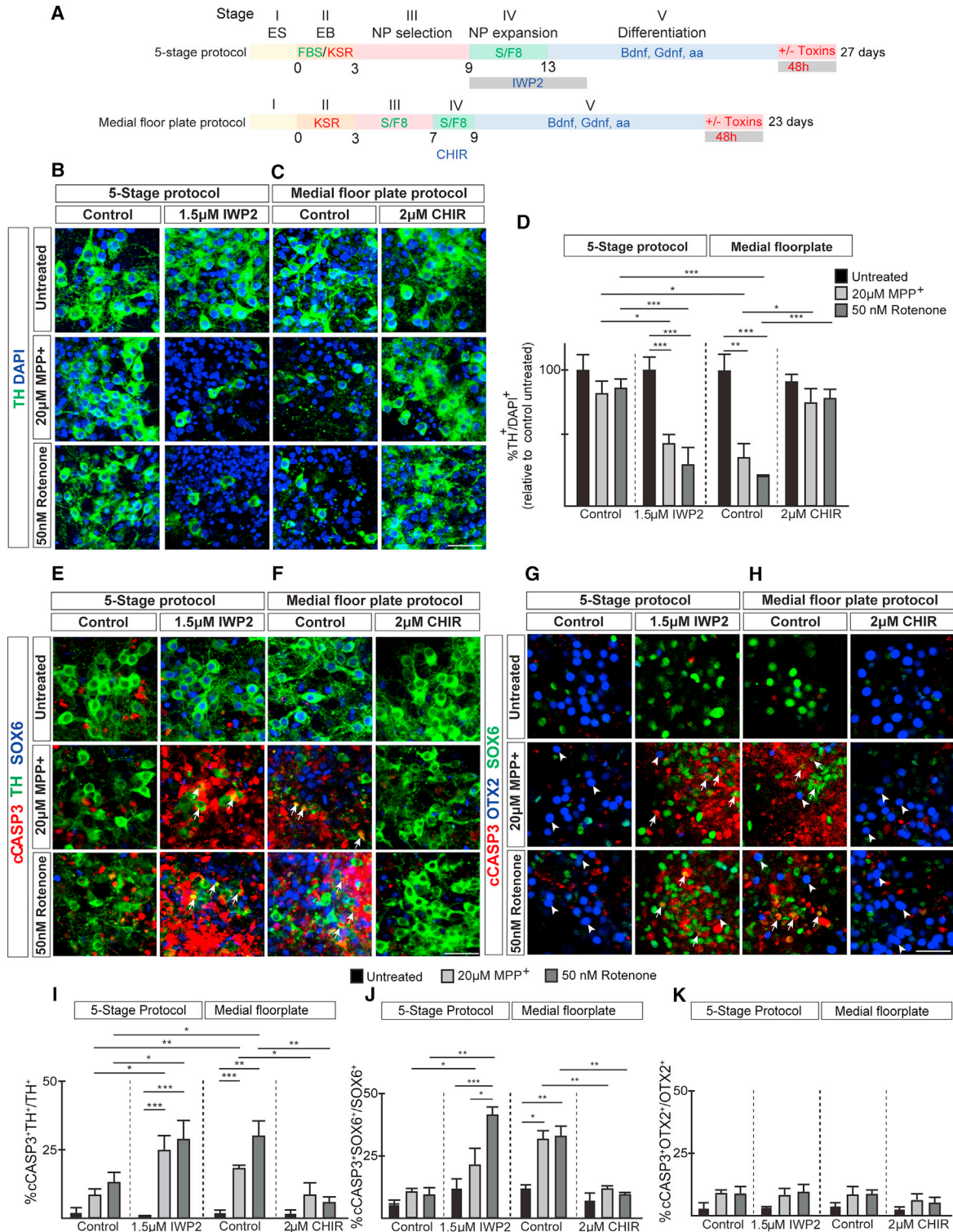*p < 0.05, **p < 0.01, ***p < 0.001. Scale bars, 50 μm.

Figure 3. Modulation of WNT signaling affects the sensitivity of neurons to mitochondrial toxins

(A) Diagram presenting the mESC differentiation conditions.

(B and C) (B) Analysis of TH in relation to DAPI in cultures differentiated according the 5-stage protocol and (C) the medial FP protocol.

(legend continued on next page)

WNT signaling inhibition directs hESC differentiation toward SN-like DA neuronal lineage

In the human fetal brain, SOX6 is expressed in SN neurons (93%) (Figures 4A and 4B), the PBP part of the VTA (Figure 6A), and the RRF (data not shown), while OTX2 is mainly confined to the VTA (Figures 4A, 4B, and 6A) except for a few labeled cells in the SN (5%). Human ESC (hESC)-derived DA neurons differentiated according to a modified version of the FP protocol (Kriks et al., 2011) were mainly expressing OTX2 and were negative for SOX6 (Figure 4C). We first addressed whether human DA progenitors, defined by LMX1A expression (Marklund et al., 2014), could be subdivided into distinct domains, analogous to the mouse. *SOX6*- and *CORIN*-labeled cells are confined to the medial progenitor domain in the CS16 human embryonic midbrain (Figure 4E). The laterally defined expression of *WNT1* (Figure 4E) suggests a role for WNT/β-CATENIN signaling in DA subpopulation specification and prompted us to investigate whether WNT inhibition promotes SN-like lineage specification also during hESC differentiation.

SHH and WNT are inducers of LMX1A and OTX2 expression, which through feedforward mechanisms enhance WNT signaling (Chung et al., 2009; Prakash et al., 2006), possibly resulting in VTA neuronal lineage-inducing culture conditions. Therefore, we decided to test the potential of IWP2 to induce SN-specific lineage markers in cultures that were exposed to different levels of SHH pathway activation and altered durations of WNT signaling, as illustrated in Figures S2A and S2F. SHH pathway activation was lowered by using Smoothened Agonist (SAG) (Figure S2F), as confirmed by reduced *GLI1* expression (Figure S3D). The window of CHIR exposure was shortened from days 4–13 to days 4–11 (referred to as CHIR and control condition, respectively; Figures 4D, S2A, and S2F), lowering the levels of canonical WNT target genes *AXIN2* and *SP5* (Figure S3E). The use of SAG and/or removal of CHIR at day 11 did not affect general aspects of DA neuron specification, with high percentages (about 75%) of LMX1A+FOXA2+ double-labeled progenitors (Figures S2D, S3A, and S3F) and LMX1A-, FOXA2-, and NR4A2-positive DA neurons observed (Figures S2E, S4A–S4C, and S4I). IWP2 was added to the cultures at or after day 11 to prevent interference with DA neuron generation in general (Figures S2A and S2F). Testing several culturing conditions (as outlined in Figures S2A and S2F), we concluded that exposure of SAG-treated control DA progenitors to 0.5 and 1 μM IWP2 between day 11 and day 16 resulted in the most robust induction of SOX6 in DA neurons (Figure S2G). Any other variation in timing and concentration of IWP2 addition resulted in less optimal outcomes (Figures S2F and S2G). Moreover, the addition of IWP2 (0.5–4 μM from day 11 to day 16/18) to DA progenitors treated with high-dose SHH did not result in the induction of any SOX6-labeled DA neurons and there was no decrease of OTX2 expression (Figures S2A, S2B, and S2D), suggesting that under these conditions progenitors lack the competence to acquire SN-like lineage characteristics in response to WNT inhibition.

Exposure of SAG-treated control DA progenitors to 0.5 and 1 μM IWP2 at days 11–16 (Figure 4D) significantly increased the percentage of SOX6-labeled DA neurons (39% with 1 μM IWP2) compared with CHIR (7%) and control (12%) conditions after 25 days. Reciprocally, the number of OTX2+ DA neurons significantly decreased under the same conditions (CHIR: 65%; control: 53%; 1 μM IWP2: 28%) (Figures 4F, 4G, S2F, and S2G). SOX6 and OTX2 expression did not overlap in DA neurons from IWP2-treated cultures (Figure 4F). Similar results were obtained with WNT antagonist DKK1 (Figure 4G). In addition, DA subpopulation-specific markers KCNJ6 (GIRK2) (Figures S4D and S4E) and CALB1 (Figure S4F) were up- and down-regulated, respectively, by IWP2 treatment (Figures S4J and S4K), consistent with acquisition of SN-like identities. The IWP2-induced SOX6-positive DA neurons coexpressed SATB1 (Figure S4G) and ALDH1A1 (Figure S4H) (Anderegg et al., 2015), further confirming their SN-specific identity. Furthermore, the use of SAG in combination with IWP2 did not compromise midbrain identity, with most progenitors LMX1A+FOXA2+ double positive (Figure S3A) and more than 70% of DA neurons coexpressing LMX1A, NR4A2, and FOXA2 under all conditions (Figures S4A, S4B, S4C, and S4I). IWP2-mediated induction of SOX6+ SN-like DA neurons was reproduced in an independent human induced PLC (iPSC) line carrying a triplication of the


(D) Graph showing the percentage of TH-expressing neurons in relation to DAPI. Mean values ± SD; two-way ANOVA with Bonferroni correction; n = 3 independent experiments.

(E and F) (E) IHC analysis of cultures differentiated according the 5-stage protocol and (F) the medial FP protocol. Arrows point to cCASP3+ TH+-labeled neurons.

(G and H) (G) IHC analysis of cultures differentiated according the 5-stage protocol and (H) the medial FP protocol. Arrows point to cCASP3+ SOX6+-labeled neurons. Arrowheads indicate OTX2+ neurons negatively labeled for cCASP3.

(I–K) Graphs showing (I) the percentage of cCASP3 in relation to TH, (J) the percentage cCASP3-expressing cells in relation to SOX6, and (K) the percentage cCASP3-expressing cells in relation to OTX2 under various culture conditions. Mean values ± SD; two-way ANOVA with Bonferroni correction; n = 3 independent experiments.

*p < 0.05, **p < 0.01, ***p < 0.001. Scale bars, 50 μm.
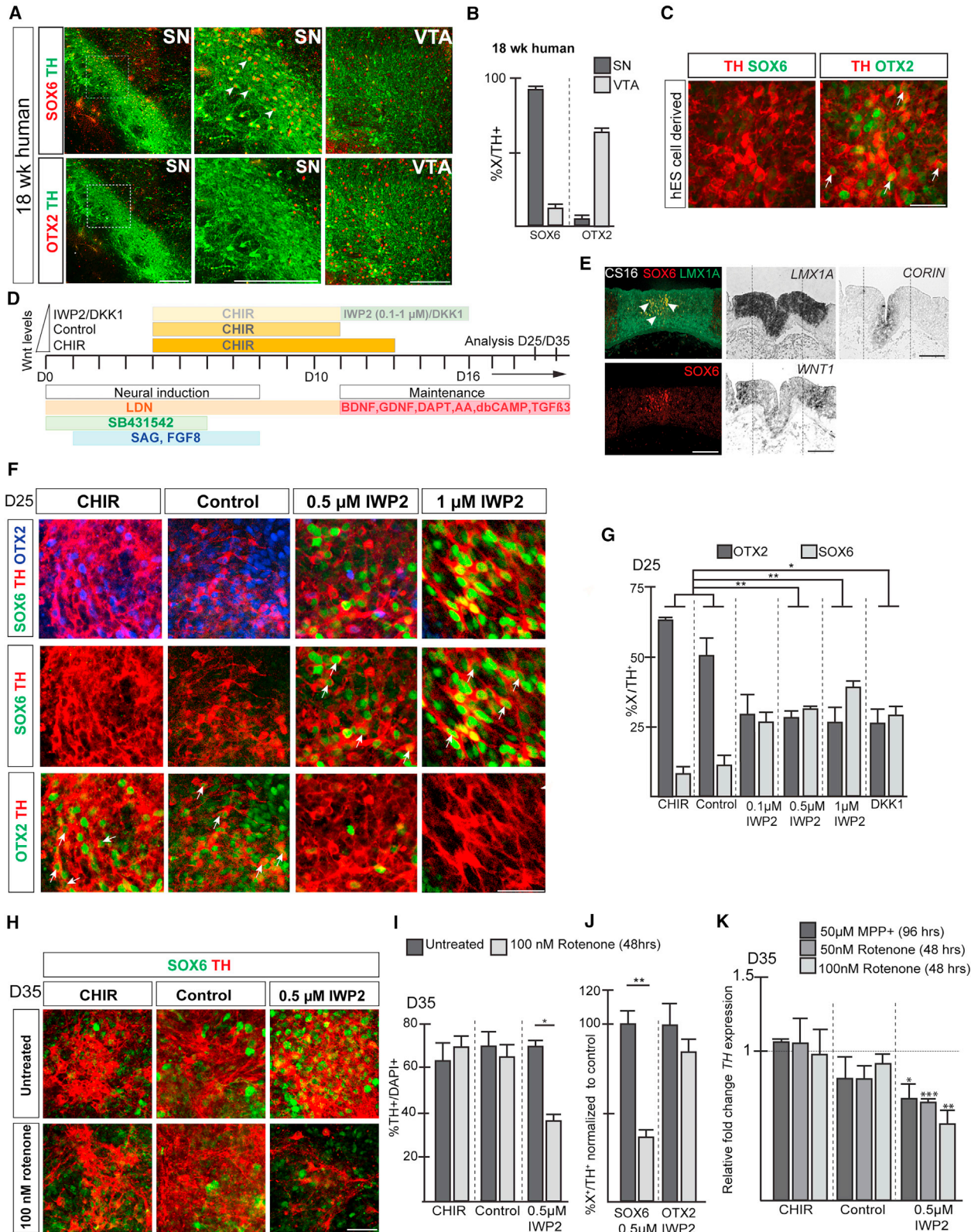
(legend on next page)

α-synuclein locus (AST) (Devine et al., 2011) (Figures S5A–S5C).

To address whether DA sublineage selection takes place at a progenitor level in human cultures, we analyzed the effect of WNT signaling modulation in DA progenitors. As expected, IWP2 treatment resulted in a downregulation of *AXIN2* and *SP5* expression at day 13 compared with control conditions, while increased levels were observed under CHIR conditions (Figure S3E). *OTX2* and *SOX6* were down- and upregulated, respectively, in DA progenitors upon IWP2 treatment (Figures S3B and S3F), consistent with the sublineage selection. While SOX6 and OTX2 were overlapping in control and CHIR-treated cultures, their expression became separate in IWP2 culture conditions. The IWP2-dependent increase of *CORIN* expression (Figures S3C and S3G) further demonstrates that the induction of medial progenitor markers correlates with the acquisition of the SN-like neuronal lineage also during human embryonic development.

We predicted that IWP2-mediated induction of SOX6 would also confer sensitivity to toxic insult. While there was only a minor effect of rotenone and MPP$^+$ in CHIR and control cultures, there was a very strong reduction in DA neurons in cultures differentiated in the presence of IWP2 (Figures 4H–4K). In particular, there was a loss of SOX6-positive DA neurons while OTX2-expressing neurons remained unaffected (Figure 4J), further demonstrating the selective sensitivity of SOX6$^+$ DA neurons to toxic insults. In agreement with the lack of Sox6 induction, IWP2 treatment did not confer sensitivity to mitochondrial toxicity in DA neurons differentiated in the presence of SHH-C24II + Pur (Figure S2C). Altogether, we demonstrate that by modulating WNT signaling levels during human PSC differentiation, we acquire distinct DA subpopulations that display selective sensitivity to mitochondrial toxins according to their identity.

Forced expression of Sox6 induces SN-like identities in human PSC-derived DA cultures

Previously, we have shown that efficient neuronal lineage induction under non-permissive culturing conditions can be achieved by overexpression of transcriptional determinants in PSC-derived progenitors (Friling et al., 2009; Panman et al., 2011). Therefore, we decided to test whether forced expression of SOX6 can induce SN neuron-specific markers also when cultures are exposed to high levels of SHH signaling. As described previously, DA neurons differentiated according to the FP protocol (Kriks et al., 2011) (Figure 5B) were mainly negative for SOX6 at day 35 (Figures 4B, 5C, and 5F), while VTA-specific markers OTX2 and CALB1 were more abundantly represented (Figures 4B, 5C, 5D, and 5F). Although SOX6 is only expressed in a small population of DA progenitors (Figures 4D [CS16] and 5A [CS20]), its expression is strongly induced in early post-mitotic neurons in a region complementary to OTX2 (Figure 5A). Consistent with these expression patterns, we transduced early post-mitotic cultures with lentiviral expression vectors for SOX6 (L-SOX6) and OTX2 (L-OTX2) at day 20 and analyzed their ability to induce DA subpopulation-specific expression at day 35 (Figure 5B). High percentages of SOX6-expressing (79%) and OTX2-expressing (75%) DA neurons were obtained upon lentiviral transduction (Figures 5C and 5F). Analysis of L-SOX6 transduced cultures revealed that a large proportion of DA neurons expressed GIRK2 (73% versus 30% in controls) (Figures 5E and 5F) and were negatively labeled for OTX2

Figure 4. WNT inhibition induces SOX6 in hESC-derived DA neurons and confers sensitivity to mitochondrial toxins

(A) IHC analysis of the human fetal brain.

(B) Percentage of SN and VTA DA neurons expressing either SOX6 or OTX2 in the human fetal midbrain.

(C) Expression of SOX6 and OTX2 in hESC-derived TH-positive neurons.

(D) Schematic overview depicting hESC differentiation conditions. CHIR (CHIR from day 4 to day 13), control (CHIR from day 4 to day 11), and IWP2 (IWP2 from day 11 until day 16).

(E) Analysis of FP markers in human embryo (cs16). Arrowheads indicate overlap of SOX6 and LMX1A expression. Dashed lines indicate medial/lateral division within progenitor domain.

(F) IHC analysis of hESC-derived cultures (day 25). Arrows point to OTX2$^+$/TH$^+$-labeled neurons in CHIR and control cultures and SOX6$^+$/TH$^+$-labeled neurons in IWP2-treated cultures. Differentiation conditions as described in (D).

(G) Percentage of TH$^+$ neurons expressing SOX6 or OTX2 differentiated as described in (D). Mean values ± SD; one-way ANOVA with Bonferroni correction; n = 4 independent experiments.

(H) Analysis of SOX6 and TH expression in hESC-derived cultures treated with rotenone for 48 h at day 35.

(I) Percentage of TH$^+$ neurons after treatment with either dimethyl sulfoxide (DMSO) or rotenone for 48 h at day 35 differentiated as described in (C). Mean values ± SD; paired t test; n = 3 independent experiments.

(J) Percentage of SOX6 or OTX2 expressing TH$^+$ neurons differentiated in the presence of IWP2 and treated with either DMSO or rotenone (100 nM) for 48 h at day 35. Mean values ± SD; paired t test; n = 3 independent experiments.

(K) Relative levels of *TH* expression in toxin-treated neurons compared with untreated (normalized to 1). Mean values ± SD; one-way ANOVA with Bonferroni correction; n = 3 independent experiments.

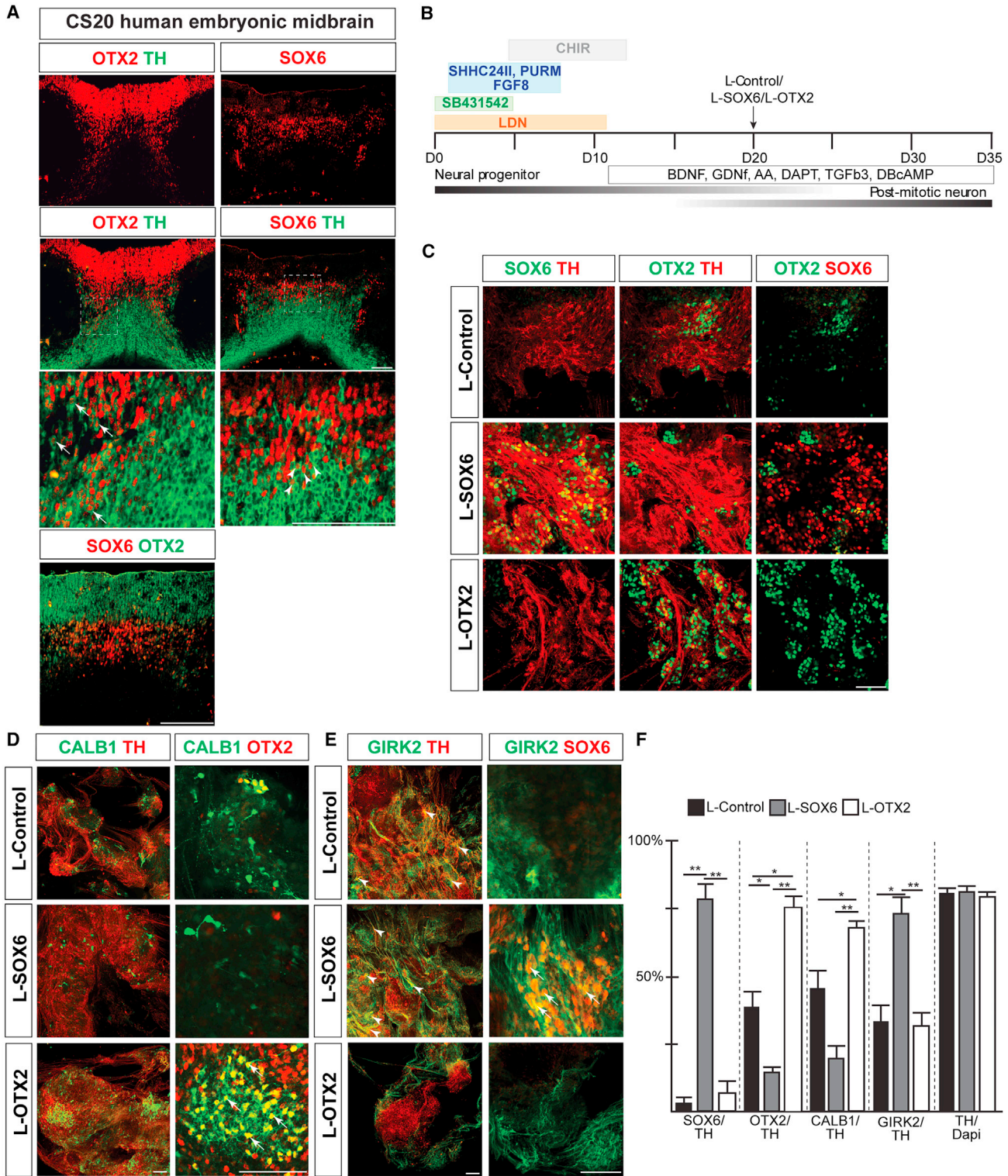*p < 0.05, **p < 0.01, ***p < 0.001. Scale bars, 200 μm (A), 100 μm (E), and 50 μm (C, F, and I).

Figure 5. Induction of DA-subpopulation-specific markers in dopaminergic cultures transduced with L-SOX6 and L-OTX2

(A) IHC analysis of coronal sections of the human embryonic midbrain. Arrows indicate OTX2+ DA neurons, while arrowheads point to SOX6+ DA neurons. Higher-magnification images are from the regions indicated by a dashed square.

(B) Schematic overview of differentiation conditions. Arrow indicates time point of lentiviral transduction.

(legend continued on next page)

(15% versus 40% in controls) (Figures 5C and 5F) and CALB1 (21% versus 41% in controls) (Figures 5D and 5F). In contrast, transduction with OTX2 resulted in an increased number of TH⁺ neurons expressing the VTA-specific marker CALB1 (67%) (Figures 5D and 5F) and a reduction of GIRK2 expression (32%) (Figures 5E and 5F). Midbrain identity (Figures S6B and S6C) and TH⁺ cell numbers (Figure 5F) remained unaffected by lentiviral overexpression. These results demonstrate that we can direct the differentiation of hESCs toward enriched cultures for mDA neurons that display either SN- or VTA-like subtype identities using lineage-specific transcription factors. In addition, similar outcomes were obtained when using the AST iPSC line (Devine et al., 2011), showing an increased expression of SOX6 and GIRK2 upon L-SOX6 transduction (Figures S5E and S5I) and a reciprocal increase of VTA-specific markers OTX2 and CALB1 with L-OTX2 (Figures S5E, S5G, and S5I). Interestingly, there was a dramatic increase in α-SYNUCLEIN (α-SYN) expression in neurons transduced with SOX6 (Figures S5F and S5H), indicating that our strategy can be used to reveal genotypic and cell-type-specific disease phenotypes in iPSCs.

Sox6 induction confers vulnerability to human PSC-derived dopaminergic neurons

To provide a further link between SOX6 induction, acquisition of SN-like identities, and selective vulnerability, we examined the effect of mitochondrial toxins on lentiviral transduced cultures. hESC-derived dopaminergic neurons transduced with either L-Control, L-SOX6, or L-OTX2 (Figure 5B) were treated with rotenone for 24 h at day 35 and assayed for cell viability. In contrast to control and L-OTX2 transduced cultures, we observed elevated levels of cCASP3 and a reduction in numbers of TH⁺ neurons in L-SOX6 transduced cultures after exposure to rotenone (Figures 6A and 6C). The difference in sensitivity between virus transduced cultures was further confirmed by the selective loss of viable cells in L-SOX6 transduced neurons, as indicated by a reduction in cellular ATP content (Figures 6D and S5J). Although higher concentrations of rotenone (100 nM) also caused a reduction of *TH* expression in control cultures as revealed by qPCR analysis, the reduction was more striking in L-SOX6 transduced neurons and not observed in L-OTX2 transduced cultures, consistent with the suggested role for OTX2 in neuroprotection (Di Salvio et al., 2010) (Figure 6E). Remarkably, in L-SOX6 transduced

cultures the number of SOX6-labeled DA neurons was drastically reduced upon rotenone treatment (Figures 6B and 6F), while OTX2 expression was maintained in L-OTX2 transduced cultures. The formation of an excess amount of reactive oxygen species (ROS) contributes to the selective degeneration of SN neurons (Dias et al., 2013). Rotenone caused a strong increase in ROS production selectively in L-SOX6 transduced cultures (Figures S6D and S6E). Similar results were obtained with the mitochondrial inhibitor MPP⁺, which is more efficiently taken up by SN neurons (Di Salvio et al., 2010). Forced expression of SOX6 in DA neurons resulted in increased sensitivity to MPP⁺ (20 μM for 96 h) with elevated levels of cCASP3 and a reduction in TH expression (Figures S6F, S6H, and S6I). cCASP3 was upregulated in the nuclei of SOX6-expressing neurons after MPP⁺ treatment, consistent with the increased susceptibility of these neurons to undergo apoptosis (Figure S6F). Consistent with the higher resistance of VTA neurons to mitochondrial toxicity, exposure to 20 μM MPP⁺ for 96 h did not have any effect on control and L-OTX2 transduced cultures (Figures S6G–S6I).

Proteins involved in metabolism are enriched in Sox6-induced SN-like neurons

To understand how SOX6 renders DA more vulnerable, we determined the protein species induced by SOX6. Therefore, DA neuronal cultures were transduced with L-Control, L-SOX6, and L-OTX2 (Figure 5B), and differences in protein expression between the cultures were determined at day 35 (Table S2) by mass spectrometry using label-free quantitative methods. We identified several proteins that are differently expressed between L-SOX6 and L-OTX2 transduced cultures (Figure 7A; fold change [FC] > 2; p < 0.05). Western blot analysis confirmed these results and showed the expected induction of SOX6 and OTX2 in L-SOX6 and L-OTX2 transduced samples, respectively (Figures S7A and S7B). Pathway analysis showed an enrichment of proteins involved in metabolism and glycolysis in L-SOX6 transduced neurons (Figure 7B), consistent with the reported higher rate of glycolysis in SN neurons needed for ATP production (Pacelli et al., 2015). The expression of the proteins involved in metabolism was further validated by *in situ* hybridization and immunohistochemistry and confirmed that VAT1, GOT1, PGAM1, glucose-6-phosphate isomerase (GPI), and ALDOC are more highly expressed in the SN of the 18-week-old human fetal or embryonic day 18.5

(C) IHC analysis of day-35 lentiviral transduced cultures.
(D) IHC analysis of lentivirus transduced cultures (day 35). Arrowheads indicate overlap between CALB1 and OTX2.
(E) IHC analysis of lentivirus transduced cultures at day 35. Arrowheads indicate overlap between GIRK2 and SOX6.
(F) Graph showing percentage of TH⁺ neurons expressing indicated markers at day 35. Mean ± SD; one-way ANOVA with Bonferroni correction; n = 3 independent experiments.
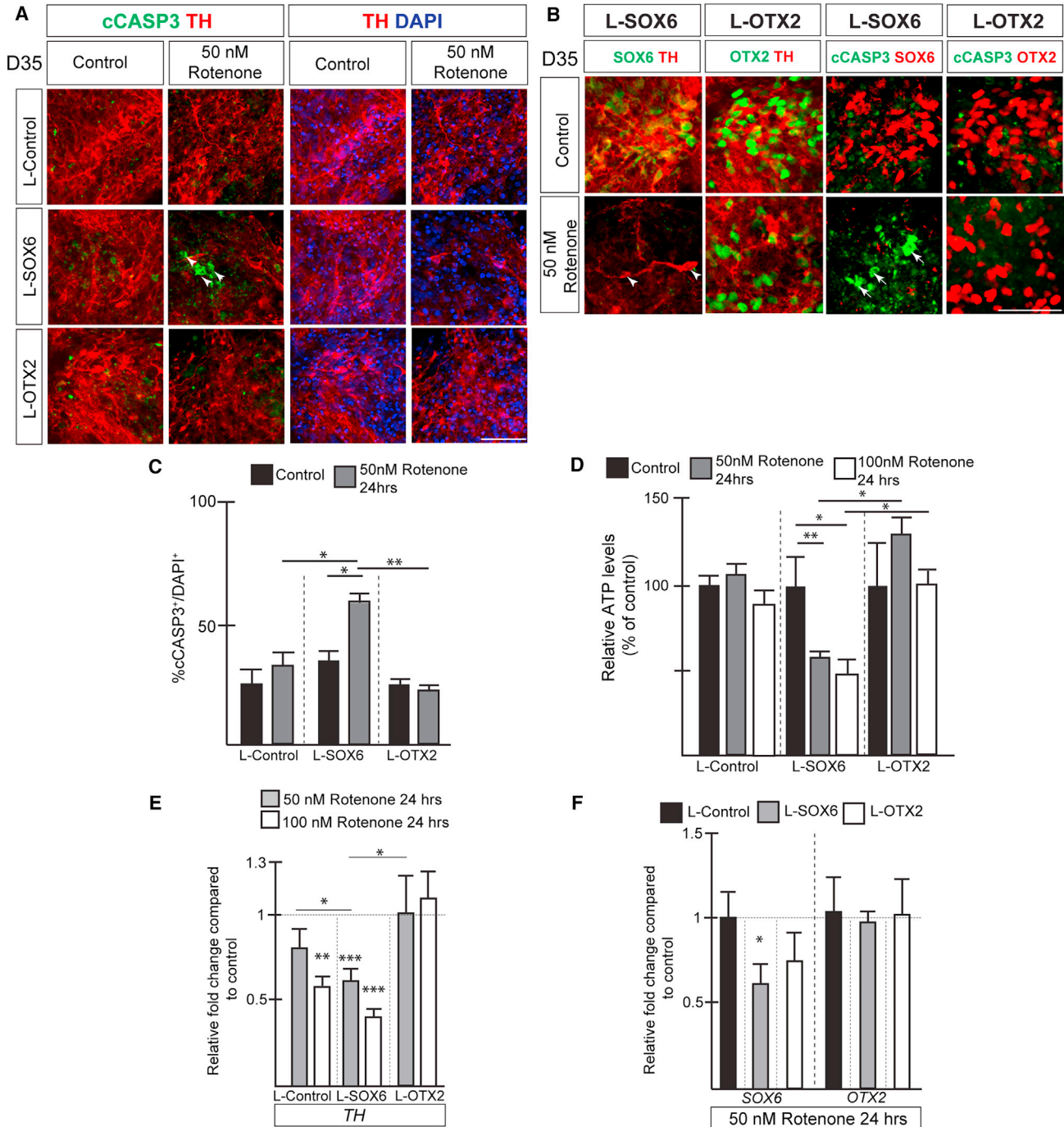*p < 0.05, **p < 0.01. Scale bars, 100 μm.

Figure 6. L-Sox6 transduced dopaminergic neurons display increased sensitivity to rotenone

(A) IHC analysis of lentiviral transduced cultures treated with rotenone at day 35 for 24 h. Arrowheads indicate cCASP3-expressing cells.

(B) Immunohistochemical analysis shows loss of SOX6 expression (arrowheads) and increase in cCASP3 (arrows) expression in L-SOX6 transduced cultures upon rotenone treatment.

(C) Graph displaying % percentage of CASP3$^+$/DAPI$^+$ in virus transduced control and 50 nM rotenone (24 h)-treated cultures at day 35. Mean ± SD; one-way ANOVA with Bonferroni correction; n = 3.

(D) Relative ATP levels in rotenone-treated cultures (24 h, day 35) as a percentage of the untreated cultures. Mean ± SD; one-way ANOVA with Bonferroni correction; n = 4 independent experiments.

(legend continued on next page)

(E18.5) mouse midbrain (Figures S7C and S7D). To gain insight into the requirement of glycolysis in SN-like DA neuron-enriched cultures, we decided to pharmacologically interfere with the levels of glycolysis. We used 6-phospho-gluconic acid (6PG), an inhibitor of GPI (Parr, 1956) and meclizine (Gohil et al., 2010), to reduce and elevate, respectively, the rate of glycolysis in hESC- and mESC-derived SN-like DA neuronal cultures. While addition of 10 μM 6PG for 24 h at day 35 had only a very minor effect on cell viability in L-SOX6 hESC-derived DA cultures (Figure 7D), its combination with 50 nM rotenone synergistically reduced the cellular ATP levels (Figure 7D), induced cCASP3 expression, and decreased the number of TH- and SOX6-positive neurons (Figure 7C). In contrast, L-Control and L-OTX2 transduced cultures were relatively unaffected after reducing both glycolysis and oxidative phosphorylation (Figure 7D). Next, we examined whether enhancement of glycolysis using meclizine protects L-SOX6 transduced cultures against mitochondrial toxicity. Remarkably, the effects of rotenone on cell survival were reversed by the addition of meclizine at the same time, decreasing the levels of cCASP3 and increasing SOX6 expression (Figures 7C and 7E). Similar effects of meclizine were obtained in mouse mFP-derived DA cultures. Rotenone treatment of SOX6-enriched DA cultures resulted in increased levels of cCASP3 (Figure 7F) and a reduction of TH$^+$ cells (Figure 7G). However, treatment with meclizine reversed the effects of rotenone on neuronal cell death, and levels of TH expression were significantly increased (Figures 7F and 7G). This comparative protein expression analysis has revealed several targetable proteins and pathways that could be used for future studies to discover novel strategies to prevent neurodegeneration.

DISCUSSION

Neurodegenerative diseases typically affect a selective population of neurons (Roselli and Caroni, 2015), and the ability to generate these disease-relevant neuronal subtypes *in vitro* will offer important opportunities for disease modeling and drug discovery. Here we showed that the differentiation of mouse and human PSC-derived DA progenitors can be directed toward the SN-like neuronal lineage either through WNT inhibitor-mediated induction of mFP cells or by forced expression of SOX6 (Figure 7H). The obtained cultures displayed the selective sensitivity of SN neurons to mitochondrial toxins, while cultures mainly consisting of DA neurons with VTA-like identities were more resistant (Figure 7H). Our approach demonstrates that the differential vulnerability of DA neurons can be reproduced in PSC-derived cultures, providing a platform for modeling PD.
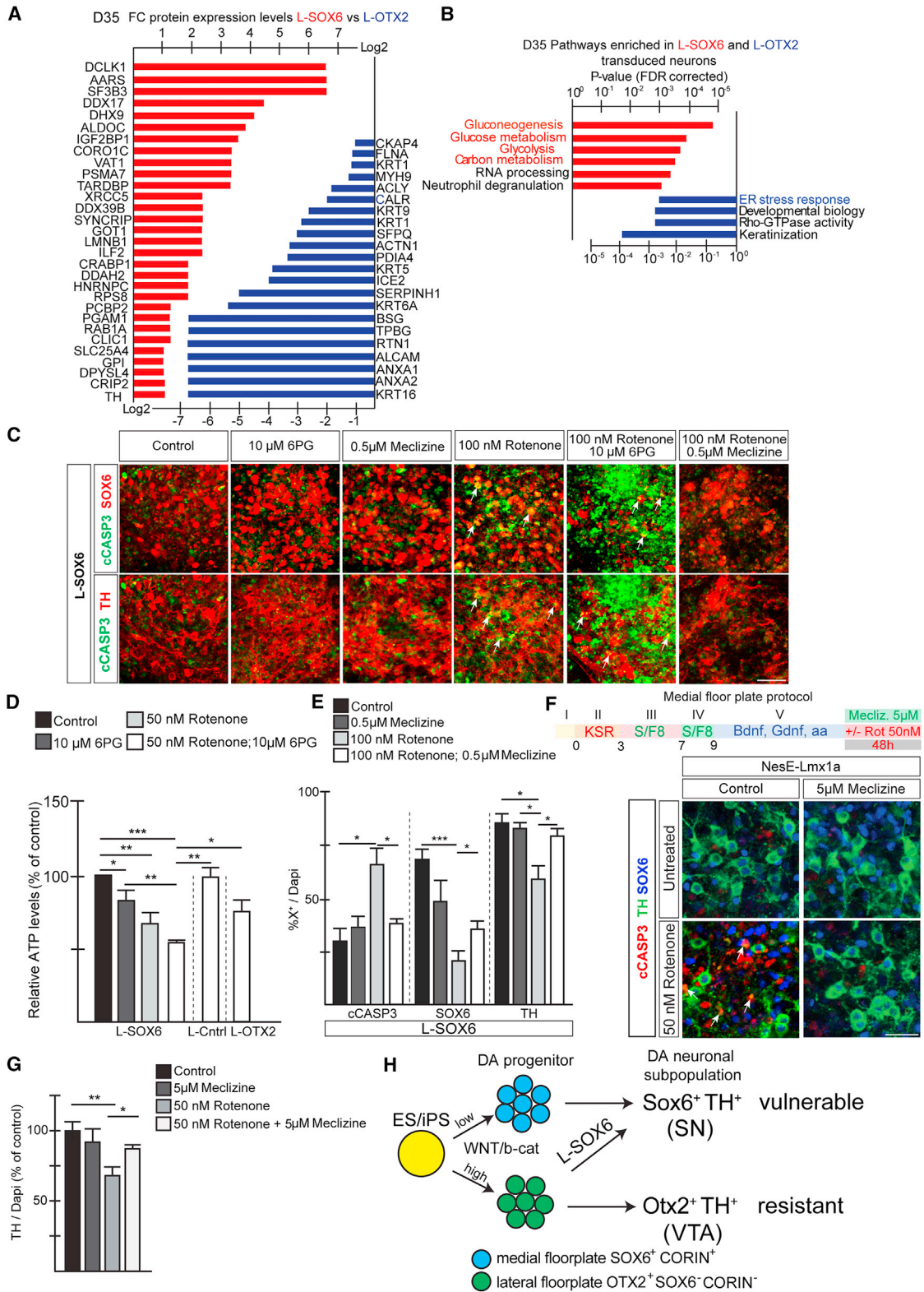
Published mouse and human PSC differentiation protocols give rise to a mixture of DA neurons with SN- and VTA-specific neuronal identities (Friling et al., 2009; Grealish et al., 2014; Kriks et al., 2011). Here we described how cultures enriched for a specific subpopulation can be obtained *in vitro*. We found that SN- and VTA-like neuronal lineages are derived from distinct DA progenitor populations during PSC differentiation, as observed during embryonic development (Blaess et al., 2011; Panman et al., 2014). mESC differentiation conditions that promoted the specification of medial progenitor (mFP) cells resulted in the efficient induction of the SN lineage-associated marker Sox6 in nearly all DA neurons. In contrast, lateral DA progenitors were generated under culture conditions that promote the specification of DA neurons with mainly VTA-like identities (Figure 7H). Consistent with mouse studies (Nouri et al., 2015; Yang et al., 2013), our data suggest that specification of these distinct lateral and medial progenitor populations is mediated by differential WNT/β-CATENIN signaling during DA progenitor differentiation. First, mESCs differentiated according to the mFP protocol, which give rise to the SN-like neuronal lineage, showed lower levels of endogenous canonical WNT signaling at the progenitor stage. Second, WNT signaling inhibition resulted in a lateral to medial switch of DA progenitor identity, which promoted the acquisition of SN-like specific identities in DA cultures. Third, activation of WNT signaling directed the differentiation toward the VTA-like neuronal lineage.

The timing and concentration of growth factor addition to PSC-derived cultures are important determinants of the differentiation outcome, as shown for several neuronal populations including cortical, motor, and serotonergic neurons (Tao and Zhang, 2016). The pleiotropic role of WNT signaling in mDA neuron development underlines the importance for defining optimal concentrations and time points for adding WNT signaling inhibitors. We defined that the critical window for IWP2-mediated induction of SOX6 in human PSC-derived DA neurons is from day 11 to day 16, once DA progenitors have been fully specified (Kriks et al., 2011). The addition of WNT inhibitors before DA progenitors have been fully specified will

(E) qPCR analysis of *TH* expression in rotenone-treated (24 h, day 35) virus transduced cultures compared with untreated cultures (normalized to 1). Mean ± SD; one-way ANOVA with Bonferroni correction; n = 4 independent experiments.

(F) qPCR analysis of *SOX6* and *OTX2* expression in rotenone-treated (24 h, day 35) virus transduced cultures compared with untreated cultures (normalized to 1). Mean ± SD; unpaired t test; n = 4 independent experiments.

*p < 0.05, **p < 0.01. Scale bars, 50 μm.

A D35 FC protein expression levels L-SOX6 vs L-OTX2

B D35 Pathways enriched in L-SOX6 and L-OTX2 transduced neurons

C

D

E

F Medial floor plate protocol

G

H

(legend on next page)

interfere with DA neuron production (Kee et al., 2017; Kirkeby et al., 2012; Kriks et al., 2011; Nolbrant et al., 2017). Extending the exposure time to IWP2 strongly reduces DA cell numbers, which is consistent with the later requirement of canonical WNT signaling for DA neuron survival (L'Episcopo et al., 2011; Zhang et al., 2015).

Although we were able to guide the mESC differentiation toward the SN-like neuronal lineage using extrinsic factors in the mFP protocol, the addition of Wnt signaling inhibitors alone did not result in a complete lineage conversion in human ESC-derived DA progenitors. Other signaling pathways, including bone morphogenetic protein, transforming growth factor α, and SHH (Blaess et al., 2011; Blum, 1998; Jovanovic et al., 2018), may cooperate with WNT in specifying subpopulation identity. Transcription factor overexpression has been successfully applied previously to overcome these hurdles and efficiently generates homogeneous neuronal populations even under non-permissive culture conditions (Au et al., 2013; Friling et al., 2009; Mazzoni et al., 2013; Mong et al., 2014; Panman et al., 2011). Indeed, forced expression of the lineage-specific transcription factor SOX6 in early human PSC-derived post-mitotic DA neurons resulted in an even more efficient induction of SN neuronal lineage markers than obtained after addition of WNT inhibitors.

In this study, the achieved enrichment for SN neuronal lineage markers conferred sensitivity to mitochondrial toxins in both mouse and human PSC-derived DA cultures, which was not observed under standard differentiation conditions. Our results demonstrate that the culture-dependent sensitivity is directly related to the molecular identity of the obtained neurons, providing a functional verification of PSC-derived DA subpopulations. Indeed, exposure to MPP$^+$ and rotenone resulted in apoptosis, reduction in ATP levels, and increased ROS production selectively in SN-like enriched cultures, consistent with in vivo models of PD. Interestingly, in particular SOX6-expressing neurons were affected upon toxin exposure with cCASP3 overlapping with SOX6 in the nucleus. This effect was reversed when levels of SOX6 were downregulated either by CHIR treatment or high-dose SHH conditions. Thus, the induced sensitivity correlated with the presence of SOX6-labeled DA neurons and was not caused by modified culture conditions. Since SN and VTA DA neurons have specialized functions and are associated with distinct neurological disorders, our platform will be highly amenable for PD disease modeling in vitro.

Comparative protein analysis between L-SOX6 and L-OTX2 transduced cultures revealed several subpopulation-specific features that could underlie the differences in vulnerability. Consistent with the higher metabolic demand of SN neurons (Bolam and Pissadaki, 2012; Pacelli et al., 2015), pathway analysis revealed an enrichment for proteins involved in glycolysis and glucose metabolism. Indeed, it has been shown previously that the glycolytic rate is higher in SN neurons compared with the VTA and is further increased after blocking mitochondrial respiration to compensate for the loss of ATP production (Chaudhuri et al., 2015; Pacelli et al., 2015). We demonstrated that blocking glycolysis with the GPI antagonist 6PG exacerbated the effects of rotenone selectively in L-SOX6 transduced cultures. Furthermore, enhancing glycolysis with meclizine (Gohil et al., 2010) prevents the induction of cCASP3 and increases cell viability in SN-like neurons after mitochondrial toxic insult. Although the molecular targets are currently unknown, meclizine is a Food and Drug Administration-approved drug crossing the blood-brain barrier and therefore may hold therapeutic potential in the treatment of PD and other neurodegenerative diseases.

Finally, our in vitro platform provides a unique approach for modeling selective neuronal vulnerability in PD and could be applied to other neurodegenerative diseases, including amyotrophic lateral sclerosis and Alzheimer's disease. It lays a framework for examining mechanisms underlying selective neuronal cell death in general and will facilitate the discovery of genes and drugs that modulate

Figure 7. SOX6-mediated induction of metabolic pathways provides protection of neurons to mitochondrial toxicity

(A) Proteins differentially expressed between L-SOX6 (red bars) and L-OTX2 (blue bars) transduced hESC-derived cultures (day 35). Expression levels are presented as $\log_2$ transformed fold change (FC) values.

(B) Graph indicates pathways significantly enriched in L-SOX6 and L-OTX2 transduced cultures.

(C) IHC analysis of L-SOX6 transduced hESC-derived cultures treated as indicated for 24 h at day 35. Arrows indicate cCASP3-labeled SOX6- and TH-expressing neurons.

(D) Relative ATP levels in rotenone- and 6PG-treated cultures (24 h, day 35) as a percentage of the untreated cultures. Mean ± SD; one-way ANOVA with Bonferroni correction; n = 4 independent experiments.

(E) Percentage of cCASP3-, SOX6-, and TH-expressing cells in hESC-derived L-SOX6 transduced cultures treated with rotenone and meclizine (24 h, day 35). Mean ± SD; one-way ANOVA with Bonferroni correction; n = 4 independent experiments.

(F) mESC differentiation scheme. IHC analysis of Nes-Lmx1a mESC-derived cultures. Arrows indicate overlap between cCASP3 and TH.

(G) Percentage of TH$^+$ neurons present in mESC medial FP-derived cultures. Control value normalized to 100. Mean ± SD; one-way ANOVA with Bonferroni correction; n = 4 independent experiments.

(H) Model illustrating DA sublineage selection process during mouse and human PSC differentiation and its consequences on vulnerability.

*p < 0.05, **p < 0.01, ***p < 0.001. Scale bars, 50 μm.

these differences in sensitivity to disease. The established differentiation protocols can be used to further explore the mechanisms controlling DA diversity during ESC differentiation using SOX6 and OTX2 in combination with other early subpopulation-specific markers.

EXPERIMENTAL PROCEDURES

Detailed descriptions of the experimental procedures can be found in the supplemental information.

Maintenance and differentiation of mouse ESCs

Wild-type E14.1 and NesE-Lmx1a mouse ESC lines were propagated on MEF cells as previously described (Friling et al., 2009; Panman et al., 2011) in the presence of LIF. Mouse ESCs were differentiated according to the 5-stage protocol as previously described (Lee et al., 2000) with some minor modifications. For the mFP protocol, basic FGF, FGF8, and SAG1.3 were added to stage III.

Maintenance and differentiation of hESCs and iPSCs

Human ESCs H9 (WA09, passage 32–48) (Thomson et al., 1998) and iPSCs AST23 (Edi001-A ECACC cat. no. 66540058, passage 25–35) (Devine et al., 2011) were cultured on Geltrex-coated 6-well plates in Essential 8 medium (Gibco) as described by the manufacturer's protocol. hESCs and iPSCs were differentiated according to the FP protocol (Kriks et al., 2011) with some minor modifications.

Quantitative mass spectrometry analysis

For each condition, three independent biological replicates were obtained. Each sample was divided over three lanes and migrated on a 10% SDS-PAGE gel. The gel was stained with Coomassie blue and each lane was subsequently cut horizontally in three bands and in-gel digested with bovine trypsin (Roche). All experiments were performed on a dual linear ion trap Fourier transform mass spectrometer.

Data and code availability

The mass spectrometry proteomics data have been deposited in the ProteomeXchange Consortium (http://www.proteomexchange.org) via the PRIDE partner repository with the dataset identifier PXD028639.

SUPPLEMENTAL INFORMATION

Supplemental information can be found online at https://doi.org/10.1016/j.stemcr.2021.09.014.

AUTHOR CONTRIBUTIONS

T.O. and L.P. conceived and designed the research project; T.O., P.G., E.M.-G., C.S., M.T., R.P., K.P., V.L., L.C.-S., U.M., and L.P. performed experiments and collected and analyzed the data; S.S. and P.H. contributed new reagents; L.P. wrote the paper. All authors provided critical comments on the manuscript and results.

CONFLICTS OF INTEREST

The authors declare no competing interests.

REFERENCES

Anderegg, A., Poulin, J.F., and Awatramani, R. (2015). Molecular heterogeneity of midbrain dopaminergic neurons—moving toward single cell resolution. FEBS Lett. *589*, 3714–3726.

Au, E., Ahmed, T., Karayannis, T., Biswas, S., Gan, L., and Fishell, G. (2013). A modular gain-of-function approach to generate cortical interneuron subtypes from ES cells. Neuron *80*, 1145–1158.

Blaess, S., Bodea, G.O., Kabanova, A., Chanet, S., Mugniery, E., Derouiche, A., Stephen, D., and Joyner, A.L. (2011). Temporal-spatial changes in Sonic Hedgehog expression and signaling reveal different potentials of ventral mesencephalic progenitors to populate distinct ventral midbrain nuclei. Neural Dev. *6*, 29.

Blum, M. (1998). A null mutation in TGF-alpha leads to a reduction in midbrain dopaminergic neurons in the substantia nigra. Nat. Neurosci. *1*, 374–377.

Bolam, J.P., and Pissadaki, E.K. (2012). Living on the edge with too many mouths to feed: why dopamine neurons die. Mov. Disord. *27*, 1478–1483.

Bove, J., Prou, D., Perier, C., and Przedborski, S. (2005). Toxin-induced models of Parkinson's disease. NeuroRx *2*, 484–494.

Chaudhuri, A.D., Kabaria, S., Choi, D.C., Mouradian, M.M., and Junn, E. (2015). MicroRNA-7 promotes glycolysis to protect against 1-methyl-4-phenylpyridinium-induced cell death. J. Biol. Chem. *290*, 12425–12434.

Chen, B., Dodge, M.E., Tang, W., Lu, J., Ma, Z., Fan, C.W., Wei, S., Hao, W., Kilgore, J., Williams, N.S., et al. (2009). Small molecule-mediated disruption of Wnt-dependent signaling in tissue regeneration and cancer. Nat. Chem. Biol. *5*, 100–107.

Chung, S., Leung, A., Han, B.S., Chang, M.Y., Moon, J.I., Kim, C.H., Hong, S., Pruszak, J., Isacson, O., and Kim, K.S. (2009). Wnt1-lmx1a forms a novel autoregulatory loop and controls midbrain dopaminergic differentiation synergistically with the SHH-FoxA2 pathway. Cell Stem Cell 5, 646–658.

Devine, M.J., Ryten, M., Vodicka, P., Thomson, A.J., Burdon, T., Houlden, H., Cavaleri, F., Nagano, M., Drummond, N.J., Taanman, J.W., et al. (2011). Parkinson's disease induced pluripotent stem cells with triplication of the alpha-synuclein locus. Nat. Commun. 2, 440.

Di Salvio, M., Di Giovannantonio, L.G., Acampora, D., Prosperi, R., Omodei, D., Prakash, N., Wurst, W., and Simeone, A. (2010). Otx2 controls neuron subtype identity in ventral tegmental area and antagonizes vulnerability to MPTP. Nat. Neurosci. 13, 1481–1488.

Dias, V., Junn, E., and Mouradian, M.M. (2013). The role of oxidative stress in Parkinson's disease. J. Parkinsons Dis. 3, 461–491.

Friling, S., Andersson, E., Thompson, L.H., Jonsson, M.E., Hebsgaard, J.B., Nanou, E., Alekseenko, Z., Marklund, U., Kjellander, S., Volakakis, N., et al. (2009). Efficient production of mesencephalic dopamine neurons by Lmx1a expression in embryonic stem cells. Proc. Natl. Acad. Sci. U S A 106, 7613–7618.

Fu, Y., Yuan, Y., Halliday, G., Rusznak, Z., Watson, C., and Paxinos, G. (2012). A cytoarchitectonic and chemoarchitectonic analysis of the dopamine cell groups in the substantia nigra, ventral tegmental area, and retrorubral field in the mouse. Brain Struct. Funct. 217, 591–612.

Gohil, V.M., Sheth, S.A., Nilsson, R., Wojtovich, A.P., Lee, J.H., Perocchi, F., Chen, W., Clish, C.B., Ayata, C., Brookes, P.S., et al. (2010). Nutrient-sensitized screening for drugs that shift energy metabolism from mitochondrial respiration to glycolysis. Nat. Biotechnol. 28, 249–255.

Grealish, S., Diguet, E., Kirkeby, A., Mattsson, B., Heuer, A., Bramoulle, Y., Van Camp, N., Perrier, A.L., Hantraye, P., Bjorklund, A., et al. (2014). Human ESC-derived dopamine neurons show similar preclinical efficacy and potency to fetal neurons when grafted in a rat model of Parkinson's disease. Cell Stem Cell 15, 653–665.

Jho, E.H., Zhang, T., Domon, C., Joo, C.K., Freund, J.N., and Costantini, F. (2002). Wnt/beta-catenin/Tcf signaling induces the transcription of Axin2, a negative regulator of the signaling pathway. Mol. Cell Biol. 22, 1172–1183.

Jovanovic, V.M., Salti, A., Tilleman, H., Zega, K., Jukic, M.M., Zou, H., Friedel, R.H., Prakash, N., Blaess, S., Edenhofer, F., et al. (2018). BMP/SMAD pathway promotes neurogenesis of midbrain dopaminergic neurons in vivo and in human induced pluripotent and neural stem cells. J. Neurosci. 38, 1662–1676.

Kee, N., Volakakis, N., Kirkeby, A., Dahl, L., Storvall, H., Nolbrant, S., Lahti, L., Bjorklund, A.K., Gillberg, L., Joodmardi, E., et al. (2017). Single-cell analysis reveals a close relationship between differentiating dopamine and subthalamic nucleus neuronal lineages. Cell Stem Cell 20, 29–40.

Kirkeby, A., Grealish, S., Wolf, D.A., Nelander, J., Wood, J., Lundblad, M., Lindvall, O., and Parmar, M. (2012). Generation of regionally specified neural progenitors and functional neurons from human embryonic stem cells under defined conditions. Cell Rep. 1, 703–714.

Kriks, S., Shim, J.W., Piao, J., Ganat, Y.M., Wakeman, D.R., Xie, Z., Carrillo-Reid, L., Auyeung, G., Antonacci, C., Buch, A., et al. (2011). Dopamine neurons derived from human ES cells efficiently engraft in animal models of Parkinson's disease. Nature 480, 547–551.

L'Episcopo, F., Serapide, M.F., Tirolo, C., Testa, N., Caniglia, S., Morale, M.C., Pluchino, S., and Marchetti, B. (2011). A Wnt1 regulated Frizzled-1/beta-Catenin signaling pathway as a candidate regulatory circuit controlling mesencephalic dopaminergic neuron-astrocyte crosstalk: therapeutical relevance for neuron survival and neuroprotection. Mol. Neurodegener. 6, 49.

Lee, S.H., Lumelsky, N., Studer, L., Auerbach, J.M., and McKay, R.D. (2000). Efficient generation of midbrain and hindbrain neurons from mouse embryonic stem cells. Nat. Biotechnol. 18, 675–679.

Marklund, U., Alekseenko, Z., Andersson, E., Falci, S., Westgren, M., Perlmann, T., Graham, A., Sundstrom, E., and Ericson, J. (2014). Detailed expression analysis of regulatory genes in the early developing human neural tube. Stem Cells Dev. 23, 5–15.

Mazzoni, E.O., Mahony, S., Closser, M., Morrison, C.A., Nedelec, S., Williams, D.J., An, D., Gifford, D.K., and Wichterle, H. (2013). Synergistic binding of transcription factors to cell-specific enhancers programs motor neuron identity. Nat. Neurosci. 16, 1219–1227.

Mong, J., Panman, L., Alekseenko, Z., Kee, N., Stanton, L.W., Ericson, J., and Perlmann, T. (2014). Transcription factor-induced lineage programming of noradrenaline and motor neurons from embryonic stem cells. Stem Cells 32, 609–622.

Nakamura, R.E., and Hackam, A.S. (2010). Analysis of Dickkopf3 interactions with Wnt signaling receptors. Growth Factors 28, 232–242.

Nolbrant, S., Heuer, A., Parmar, M., and Kirkeby, A. (2017). Generation of high-purity human ventral midbrain dopaminergic progenitors for in vitro maturation and intracerebral transplantation. Nat. Protoc. 12, 1962–1979.

Nouri, N., Patel, M.J., Joksimovic, M., Poulin, J.F., Anderegg, A., Taketo, M.M., Ma, Y.C., and Awatramani, R. (2015). Excessive Wnt/beta-catenin signaling promotes midbrain floor plate neurogenesis, but results in vacillating dopamine progenitors. Mol. Cell Neurosci. 68, 131–142.

Pacelli, C., Giguere, N., Bourque, M.J., Levesque, M., Slack, R.S., and Trudeau, L.E. (2015). Elevated mitochondrial bioenergetics and axonal arborization size are key contributors to the vulnerability of dopamine neurons. Curr. Biol. 25, 2349–2360.

Panman, L., Andersson, E., Alekseenko, Z., Hedlund, E., Kee, N., Mong, J., Uhde, C.W., Deng, Q., Sandberg, R., Stanton, L.W., et al. (2011). Transcription factor-induced lineage selection of stem-cell-derived neural progenitor cells. Cell Stem Cell 8, 663–675.

Panman, L., Papathanou, M., Laguna, A., Oosterveen, T., Volakakis, N., Acampora, D., Kurtsdotter, I., Yoshitake, T., Kehr, J., Joodmardi, E., et al. (2014). Sox6 and Otx2 control the specification of substantia nigra and ventral tegmental area dopamine neurons. Cell Rep. 8, 1018–1025.

Parr, C.W. (1956). Inhibition of phosphoglucose isomerase. Nature *178*, 1401.

Poulin, J.F., Zou, J., Drouin-Ouellet, J., Kim, K.Y., Cicchetti, F., and Awatramani, R.B. (2014). Defining midbrain dopaminergic neuron diversity by single-cell gene expression profiling. Cell Rep. *9*, 930–943.

Poulin, J.F., Gaertner, Z., Moreno-Ramos, O.A., and Awatramani, R. (2020). Classification of midbrain dopamine neurons using single-cell gene expression profiling approaches. Trends Neurosci. *43*, 155–169.

Prakash, N., Brodski, C., Naserke, T., Puelles, E., Gogoi, R., Hall, A., Panhuysen, M., Echevarria, D., Sussel, L., Weisenhorn, D.M., et al. (2006). A Wnt1-regulated genetic network controls the identity and fate of midbrain-dopaminergic progenitors in vivo. Development *133*, 89–98.

Reyes, S., Fu, Y., Double, K., Thompson, L., Kirik, D., Paxinos, G., and Halliday, G.M. (2012). GIRK2 expression in dopamine neurons of the substantia nigra and ventral tegmental area. J. Comp. Neurol. *520*, 2591–2607.

Ribeiro, D., Ellwanger, K., Glagow, D., Theofilopoulos, S., Corsini, N.S., Martin-Villalba, A., Niehrs, C., and Arenas, E. (2011). Dkk1 regulates ventral midbrain dopaminergic differentiation and morphogenesis. PLoS One *6*, e15786.

Roselli, F., and Caroni, P. (2015). From intrinsic firing properties to selective neuronal vulnerability in neurodegenerative diseases. Neuron *85*, 901–910.

Smidt, M.P., and Burbach, J.P. (2007). How to make a mesodiencephalic dopaminergic neuron. Nat. Rev. Neurosci. *8*, 21–32.

Surmeier, D.J., Obeso, J.A., and Halliday, G.M. (2017). Selective neuronal vulnerability in Parkinson disease. Nat. Rev. Neurosci. *18*, 101–113.

Tao, Y., and Zhang, S.C. (2016). Neural subtype specification from human pluripotent stem cells. Cell Stem Cell *19*, 573–586.

Thomson, J.A., Itskovitz-Eldor, J., Shapiro, S.S., Waknitz, M.A., Swiergiel, J.J., Marshall, V.S., and Jones, J.M. (1998). Embryonic stem cell lines derived from human blastocysts. Science *282*, 1145–1147.

Tiklova, K., Bjorklund, A.K., Lahti, L., Fiorenzano, A., Nolbrant, S., Gillberg, L., Volakakis, N., Yokota, C., Hilscher, M.M., Hauling, T., et al. (2019). Single-cell RNA sequencing reveals midbrain dopamine neuron diversity emerging during mouse brain development. Nat. Commun. *10*, 581.

Yang, J., Brown, A., Ellisor, D., Paul, E., Hagan, N., and Zervas, M. (2013). Dynamic temporal requirement of Wnt1 in midbrain dopamine neuron development. Development *140*, 1342–1352.

Ying, Q.L., Stavridis, M., Griffiths, D., Li, M., and Smith, A. (2003). Conversion of embryonic stem cells into neuroectodermal precursors in adherent monoculture. Nat. Biotechnol. *21*, 183–186.

Ying, Q.L., Wray, J., Nichols, J., Batlle-Morera, L., Doble, B., Woodgett, J., Cohen, P., and Smith, A. (2008). The ground state of embryonic stem cell self-renewal. Nature *453*, 519–523.

Zhang, J., Gotz, S., Vogt Weisenhorn, D.M., Simeone, A., Wurst, W., and Prakash, N. (2015). A WNT1-regulated developmental gene cascade prevents dopaminergic neurodegeneration in adult En1(+/-) mice. Neurobiol. Dis. *82*, 32–45.